sciendo

CAIM
ISSN 2038-0909

Commun. Appl. Ind. Math. 15 (2), 2024, 8–16 DOI: 10.2478/caim-2024-0008

Research Article

A Weierstrass approach to the analysis of rarefaction solitary waves in tensegrity mass-spring systems

Julia de Castro Motta[1] , Luca Placidi[2], Rana Nazifi Charandabi[3], Fernando Fraternali[1*]

[1]Department of Civil Engineering, University of Salerno, Via Giovanni Paolo II, 132 - 84084 Fisciano (SA), Italy.

[2]International Telematic University Uninettuno, 00186 Rome, Italy.

[3]Department of Information Engineering, Electrical Engineering and Applied Mathematics (DIEM), University of Salerno, Via Giovanni Paolo II, 132 - 84084 Fisciano (SA), Italy.

[*]Email address for correspondence: f.fraternali@unisa.it

Communicated by Renato Spigler

Received on 05 20, 2024. Accepted on 07 31, 2024.

Abstract

The Weierstrass‘ theory of one-dimensional Lagrangian systems and a quasi-continuum approach are employed to study the propagation of solitary waves in tensegrity mass-spring chains, which exhibit softening-type elastic response in the large displacement regime and are subject to external pre-compression. The presented study analytically derives the shape of the traveling rarefaction pulses, and limiting values of the speeds of such pulses. Use is made of a tensegrity-like interaction potential that captures the main features of the real force-displacement response of the examined units. The Weierstrass approach is validated through numerical applications that establish comparisons between the theory developed in the present work and previous results available in literature.

Keywords: `Tensegrity, Solitary waves, Rarefaction pulses, Weierstrass' theory`

1. Introduction

Tensegrity structures are formed by networks of tensile members (cables) linked to compressive members (bars). These structures are not only lightweight but are also significantly tunable, presenting stiffness properties that can be adjusted by changing mechanical, geometrical, and prestress variables [1–3]. The geometrically-nonlinear response of minimal tensegrity prisms formed by three bars (T3 units) and truncated tensegrity octahedrons has been employed to show that mass-springs systems formed by such units support the propagation of solitary waves with tunable wave width [4–8]. Stiffening-type units have been shown to support the propagation of compression solitary waves [4–6], while softening-type units have been employed to form systems traversed by rarefaction solitary pulses, which are able to suitably reduce an initial state of external pre-compression of the system [7,8]. Compression solitary pulses can be profitably used to fabricate novel acoustic lenses with tunable focus [9], while rarefaction pulses can be employed to develop next-generation impact mitigation devices that do necessarily rely on energy dissipation phenomena [7].

This paper applies the nonlinear tensegrity-like potential proposed in [6] to develop a Weierstrass approach [5,6] to the existence and properties of rarefaction solitary waves in pre-compressed chains of minimal tensegrity regular prisms with softening response [7]. The presented study includes analytic formulae for the wave speed range that supports such waves, as well as an analytic description of the shape of the rarefaction pulses. A different approach has been followed in [6], making use of a more standard, quadratic approximation to the force-displacement response of tensegrity prisms with softening-type behavior. The paper is organized as follows. Section 2 describes the tensegrity-like interaction potential used to model the mechanical response of the analyzed tensegrity prisms units. The quasi-continuum limit of the equations of motion of chains of softening tensegrity prisms alternating with lumped masses are presented in Sect.3, while the Weierstrass' analysis of the solitary pulses traveling in such systems is presented in Sect. 4. Section 5 illustrates some numerical simulations that establish comparisons between

the predictions of the present theory and the results presented in [7]. The paper ends in Sect. 6 with the presentation of some concluding remarks and directions for future research.

2. A nonlinear tensegrity-like interaction potential

The present section analyzes the following tensegrity-like potential to capture the main features of the axial response law of T3 prisms

$$V(u) \;=\; \alpha_1\, u^2\, \frac{\alpha_2+u}{\alpha_3+u} \tag{1}$$

In Eqn. (1), V is the elastic potential of the prism, u is the relative axial displacement between the terminal bases, assumed positive in compression, while the quantities α_1, α_2 and α_3 represent constitutive parameters. The above potential has already been employed in [6] to describe the stiffening-type response of chains of truncated tensegrity octahedrons. We will show in short that it is also able to describe a softening response, under a suitable identification of the constitutive parameters. The constitutive response relating the (compression) axial force F acting to the terminal bases of the prism to the axial displacement u is obtained as follows

$$F(u) = \frac{dV}{du} = -\frac{\alpha_1 u^2(\alpha_2+u)}{(\alpha_3+u)^2} + \frac{\alpha_1 u(2\alpha_2+3u)}{\alpha_3+u} \tag{2}$$

and for the axial stiffness coefficient k one gets

$$k(u) = \frac{dF}{du} = \frac{2\alpha_1 u^2(\alpha_2+u)}{(\alpha_3+u)^3} - \frac{2\alpha_1 u(2\alpha_2+3u)}{(\alpha_3+u)^2} + \frac{\alpha_1(2\alpha_2+5u)}{\alpha_3+u} \tag{3}$$

The (initial) tangent stiffness k_0, for $u=0$, is easily computed as follows

$$k_0 \;=\; 2\,\frac{\alpha_1\alpha_2}{\alpha_3}. \tag{4}$$

Eqn.(3) shows that $k(u)$ tends to a horizontal asymptote $k=k_f$ for $u\to\infty$, with k_f given by

$$k_f \;=\; 2\,\alpha_1 \;=\; \frac{\alpha_3}{\alpha_2}\,k_0 \tag{5}$$

The same equation reveals that it is possible to model a softening-type response when it results in $\alpha_1>0$, $\alpha_2\geq 0$, $0<\alpha_3/\alpha_2<1$. In the special case with $\alpha_2=0$, one in particular gets $k_0=0$, that is, a model with zero initial stiffness (absence of external and internal prestress, cf. [7]). Fig. 1(a, b, c) visually illustrate the V vs. u, F vs. u and k vs. u laws, derived from Eqns.(1)-(3), for specific values of the constitutive parameters α_1, α_2 and α_3. The green and the red curves correspond to softening-type responses, while the blue curves refer to a stiffening-type behavior, which is included for the sake of comparison with the results presented in [6]. Let us introduce the strain variable $\xi = u/h_0$, and rewrite the potential (1) as follows

$$\hat{V}(\xi) \;= V(u(\xi)) \;=\; \hat{\alpha}_1\,\xi^2\,\frac{\xi+\hat{\alpha}_2}{\xi+\hat{\alpha}_3}. \tag{6}$$

where

$$\hat{\alpha}_1 \;=\alpha_1\,h_0^2, \quad \hat{\alpha}_2 \;=\; \frac{\alpha_2}{h_0}, \quad \hat{\alpha}_3 \;=\; \frac{\alpha_3}{h_0} \tag{7}$$

We now move on to fit the tensegrity-like model to the response of a micro-scale T3 prism analyzed in [7], which is composed of bars additively manufactured using the Ti6Al4V titanium alloy (0.80 mm diameter, 120 MPa Young modulus) and Spectra fiber cables (0.28 mm diameter, 5.48 MPa Young modulus). Such a prism exhibits a height of 5.63 mm in the undeformed configuration under zero external

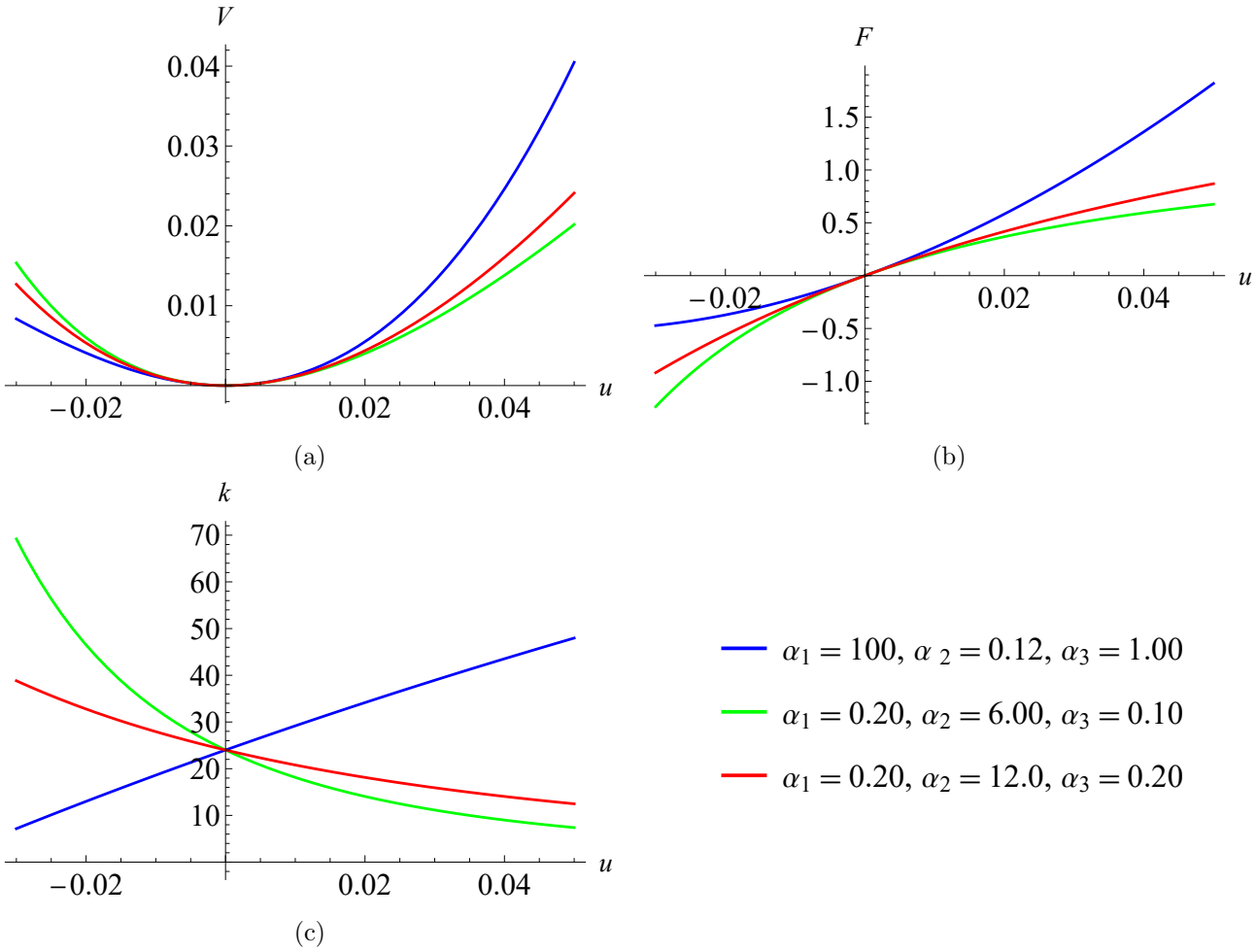

Figure 1: Plots of the interaction potential (a), axial force (b) and axial stiffness response laws of the tensegrity-like model for given values of α_1, α_2 and α_3.

force, and is supposed to be subject to a initial pre-compression force $F_0 = 31.70$ N that produces an initial compression strain $\epsilon_0 = 0.15$. Let u be identified with the axial displacement measured from the pre-compressed configuration of the prism, and let $\bar{u}$ denote the axial displacement measured from the undeformed configuration. Furthermore, let $\bar{F}_{tens}$ denote the axial force acting in the current deformation of the prism and set $F_{tens} = \bar{F}_{tens} - F_0$. Fig. 2 shows the $\bar{F}_{tens}$ vs. $\bar{u}$ and the F_{tens} vs. u laws numerically obtained for the T3 prism under examination, which show a tangent slope decreasing with the axial displacement, that is, an elastically-softening response.

Employing a set of 44 fitting points spaced along the u-axis of the F_{tens} vs. u curve, for $u \in [-1.15, 1.15]$ mm, we were able to fit the tensegrity-like model to the response depicted in Fig. 2(d), obtaining the following best fit parameters: $\alpha_1 = 5.607 \times 10^{-3}$ N/m, $\alpha_2 = 8.485 \times 10^{3}$ m and $\alpha_3 = 4.855 \times 10^{-3}$ m (use was made of the *Mathematica*® v.13.2 function 'FindFit'). Fig. 3 shows a very good matching between the tensegrity-like model and the $F_{tens} - u$ response.

3. Quasi-continuum limit of the equations of motion

The present section develops the quasi-continuum limit of the equations of motion of a mass-spring chain equipped with T3 prisms that feature an interaction law described by Eqn. (1). We analyze a chain composed of an infinitely large number of units and we let u_{i-1}, u_i and u_{i+1} denote the displacements exhibited by the masses $i-1$, i and $i+1$, respectively. The equation of motion of the i-the mass in the

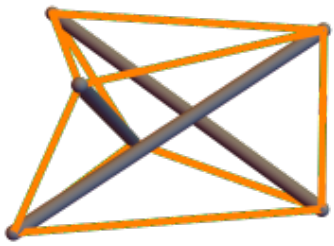

(a) Tensegrity unit under $\bar{u} = 0$

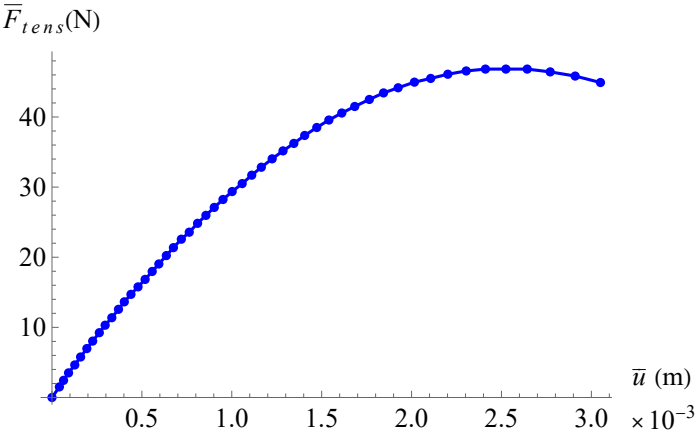

(b) $\bar{F}_{tens}$ vs. $\bar{u}$ plot

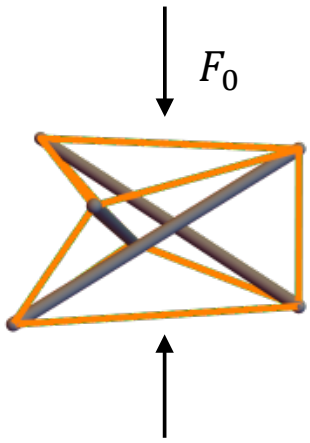

(c) Tensegrity unit under $u = 0$

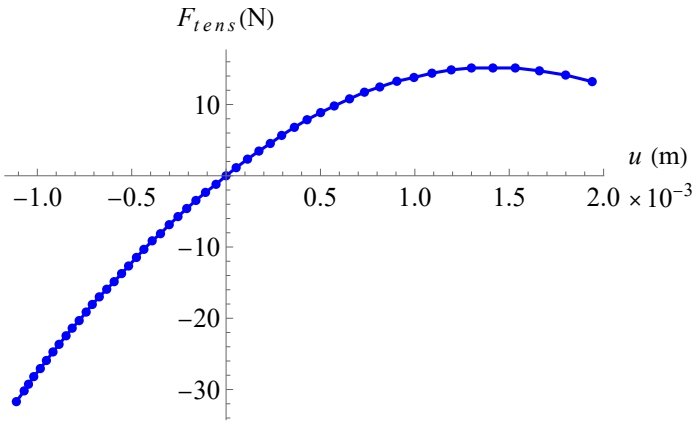

(d) F_{tens} vs. u plot

Figure 2: Force-displacement responses of T3 prisms with elastically softening behavior [7].

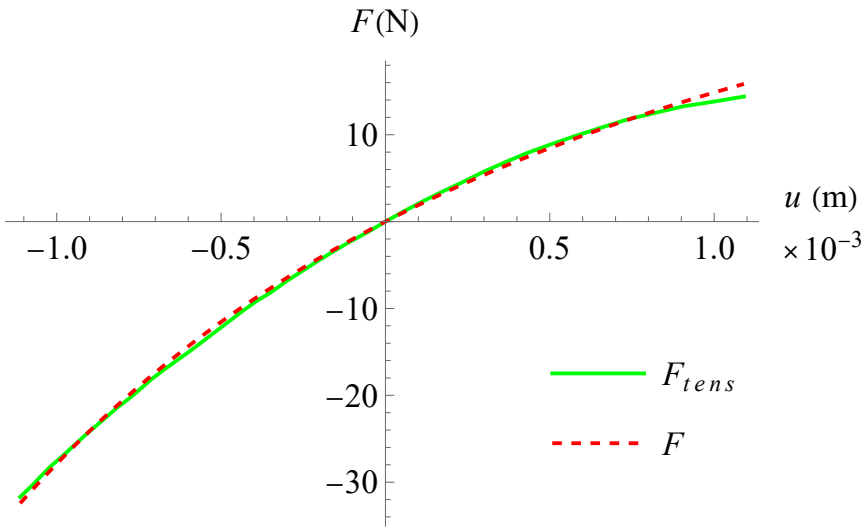

Figure 3: Fitting of the tensegrity-like model (red dashed curve) to the F_{tens} vs. u response (green-solid curve).

longitudinal direction is written as follows

$$m\ddot{u}_i = V_u\left(u_{i-1} - u_i\right) - V_u\left(u_i - u_{i+1}\right) \tag{8}$$

By introducing a longitudinal coordinate x along the axis of the chain, we now write the displacement of the i-th mass the realization of a continuous function $u(x,t)$ in correspondence to the current time t and the initial position x_i of such a mass (i.e., $u_i = u(x_i,t)$). Next, we use a discrete-to-continuum approach, which consists of employing fourth-order Taylor series expansions for $V_u\left(u_{i-1} - u_i\right)$ and $V_u\left(u_i - u_{i+1}\right)$ into Eqn. (8).

$$\frac{m}{h_0^2}u_{tt} = \mathcal{L}\{[V_u(u(x,t))]_{xx}\}, \tag{9}$$

where $\mathcal{L} \approx 1 + \frac{1}{12}h_0^2\partial_{xx}$ is a differential operator.

By considering $\epsilon << 1$ and $u \sim \epsilon u$, the Taylor expansion of Eqn. (1) with respect to ϵ is given by

$$V(u) \approx \alpha_1\frac{\alpha_2}{\alpha_3^3}\epsilon^2u^2 - \alpha_1\frac{\alpha_2-\alpha_3}{\alpha_3^4}\epsilon^3u^3 + \ldots,. \tag{10}$$

We shall now introduce this approximation in Eqn. (9). As we are dealing with a quasi-continuum approximation, where h_0 can be considered small, we can neglect the terms of order greater than $\mathcal{O}(\epsilon^3h_0^2)$. We end up with the Boussinesq equation

$$u_{tt} = \frac{h_0^2}{m}\left(\frac{\alpha_1\alpha_2}{\alpha_3}u_{xx} - 3\alpha_1\frac{\alpha_2-\alpha_3}{\alpha_3^2}(u^2)xx\right) + \gamma uxxxx, \tag{11}$$

where

$$\gamma = \frac{h_0^4\alpha_1\alpha_2}{6\alpha_3 m} \tag{12}$$

This equation allows us to use the well-known sech-^{2} solution of the Boussinesq Equation [10]. However, if we do not want to assume any approximation on the form of the potential, we can use Rosenau's [11] idea to invert the operator $\mathcal{L}$, obtaining

$$\mathcal{L}^{-1} \approx \left(1 - \frac{1}{12}h_0^2\partial_{xx}\right)$$

Applying such an inverse operator in Eqn. (9), we arrive at the following modified Boussinesq Equation

$$u_{tt} = \frac{{h_0}^2}{m}\left[V_u\right]_{xx} + \frac{1}{12}\,u_{xxtt} \tag{13}$$

The advantage of equation (13), over the more standard equation (11), is that it is well-posed mathematically. Additionally, it allows us to preserve the form of the elastic potential proposed in the present work.

It is useful to introduce the following modified potential, which is a function of the dimensionless variable ξ introduced in the previous section

$$\tilde{V}(\xi) \;=\; \frac{\hat{V}(\xi)}{m} \;=\; \tilde{\alpha}_1\,\xi^2\frac{\tilde{\alpha}_2+\xi}{\tilde{\alpha}_3+\xi}, \tag{14}$$

with

$$\tilde{\alpha}_1 = \frac{\hat{\alpha}_1}{m} = \frac{\alpha_1{h_0}^2}{m}; \quad \tilde{\alpha}_2 = \hat{\alpha}_2; \quad \tilde{\alpha}_3 = \hat{\alpha}_3 \tag{15}$$

A simple manipulation of Eqn. (13), with the aid of Eqn. (14), leads us to the differential equation

$$\xi_{tt} = \left[\tilde{V}_\xi\right]_{xx} + \frac{1}{12}\,\xi_{xxtt} \tag{16}$$

We now consider a ξ-wave traveling with speed v, by setting $\xi = \phi(x - vt)$, where ϕ is a scalar function to be determined. By restricting our attention to cases in which the rarefaction pulse does not produce the complete loss of the initial pre-compression of the system, we rquire that it results in $\phi \in [\xi_{lim}, 0]$, where $\xi_{lim} = -u_0/h_0$. Using the change of variable $z = x - vt$ and the prime notation for the differentiation with respect to z, we rewrite Eqn. (16) as follows

$$v^2\phi'' = \left[\tilde{V}_\phi\right]'' + v^2\frac{1}{12}\,\phi'''', \tag{17}$$

A double integration of Eqn. (17) with respect to z and the use of asymptotic boundary conditions leads us to write

$$v^2\frac{1}{12}\,\phi'' = v^2\phi - \left[\tilde{V}_\phi\right]. \tag{18}$$

Multiplying Eqn. (18) by ϕ' on both sides and carrying a new integration with respect to z, we finally obtain

$$\mathcal{F} = \frac{1}{v^2}\left(v^2\phi^2 - 2\tilde{V} + C\right), \tag{19}$$

where C is an integration constant, and we have set

$$\mathcal{F} = \frac{1}{12}\,\phi'^2. \tag{20}$$

which easily shows us that it results in $\mathcal{F} \geq 0$ for any $\phi \in [\xi_{lim}, 0]$.

4. Weierstrass analysis of solitary pulses

We adopt the methodology outlined [5,6] to construct a Weierstrass analysis of the solutions of Eqn. (19) [12,13]. By substituting Eqn. (14) into Eqn. (19) and setting the integration constant C to zero, we can write

$$\mathcal{F} = \phi^2\left[1 - \frac{2}{v^2}\,\tilde{\alpha}_1\frac{\tilde{\alpha}_2 + \phi}{\tilde{\alpha}_3 + \phi}\right]. \tag{21}$$

According to Weierstrass' theory, we can relate the existence of solitary pulses to the presence of two asymptotic points and an inversion point of ϕ [12,13], where it results $\phi' = 0$. Eqn. (20) show that these points actually coincide with zero points of $\mathcal{F}$. On the other hand, Eqn. (21) shows that the points where $\phi = 0$ are zero points of order two for $\mathcal{F}$, that is, asymptotic points of the wave profile. As ϕ approaches zero, it is clear from Eqn. (21) that the limitation $\mathcal{F} \geq 0$ implies that the wave speed v must be greater than the following lower bound

$$v_{min} = \sqrt{2\tilde{\alpha}_1\frac{\tilde{\alpha}_2}{\tilde{\alpha}_3}} = c_0, \tag{22}$$

where $c_0 = h_0\sqrt{\frac{k_0}{m}}$ denotes the speed of sound in the linear response regime [14].

We shall call $\phi = \phi^*$ the inversion point of the solitary pulse, which is computed by setting to zero the term in square brackets on the right hand side of Eqn. (21), obtaining

$$\phi^* = \frac{\tilde{\alpha}_3 v^2 - 2\tilde{\alpha}_1\tilde{\alpha}_2}{2\tilde{\alpha}_1 - v^2}. \tag{23}$$

Since we are studying a softening regime with $\alpha_2 > \alpha_3$ (see Sect. 2), we observe from Eqn. (23) that it result $\phi^* < 0$ (negative wave peak) in the present case. Such a noticeable result implies that the solitary pulse supported by the system under consideration is actually a rarefaction pulse, which reduces its initial state of pre-compression. By setting $\phi^* = \xi_{lim}$ in Eqn. (23), we obtain the maximum wave speed v_{max} at which the rarefaction wave can propagate, while the system remains in a compressed state. It is an easy task to obtain for such wave speed the following expression

$$v_{max} = \sqrt{2\tilde{\alpha}_1 \frac{\tilde{\alpha}_2 + \xi_{lim}}{\tilde{\alpha}_3 + \xi_{lim}}}. \tag{24}$$

We shall now determine the wave form of the solitary pulse, by introducing the inverse function $f = \pm z$. From Eqn. (20), we deduce $\frac{d\phi}{dz} = \sqrt{12\mathcal{F}}$, which allow us to write

$$f := \int \sqrt{\frac{1}{12\ \mathcal{F}}} d\phi \tag{25}$$

The insertion of Eqn. (21) into Eqn. (25) leads, after some calculations, to the following result

$$f = \frac{v}{\sqrt{3}} \frac{\psi \tan^{-1}\left(\frac{\chi}{\rho}\right) - \rho \tan^{-1}\left(\frac{\chi}{\psi}\right)}{\psi\rho} \tag{26}$$

where

$$\chi = \sqrt{v^2 - 2\tilde{\alpha}_1 \frac{\phi + \tilde{\alpha}_2}{\phi + \tilde{\alpha}_3}}, \qquad \rho = \sqrt{{c_0}^2 - v^2}, \qquad \psi = \sqrt{2\tilde{\alpha}_1 - v^2} \tag{27}$$

We will see in the next section that a simple reversal of the axes of the graph of $f(\phi)$ allows us to visualize the shape of the pulse $\phi(f)$.

5. Numerical applications

We now compare the predictions of the tensegrity-like model presented in the previous section with the numerical results obtained in [7] for the propagation of rarefaction pulses in a chain formed by 1400 T3 prisms exhibiting the properties analyzed in in Sect. 2. Such prisms are alternated with lead discs showing 2 mm thickness and 25 g mass. Let $\bar{h} = 7.63$ mm denote the undeformed height of the unit formed by a T3 prism and a lead disc, and let $\bar{\xi} = \bar{u}/\bar{h} = \xi + \epsilon_0(1-\xi)$ denote the total axial strain of the unit. We computed the wave speeds and wave width of the tensegrity-like model making use of Eqn. (23), and assuming a cutoff of ξ equal to 0.02 ϵ_0. Comparisons between the predictions of the tensegrity-like model and the numerical solutions obtained in [7] are presented in Tab. 1, considering both the speed and the width of the traveling pulses in the mass-spring chain under consideration. A good matching can be observed between the two analyzed approaches. The waveform of the tensegrity-like pulses is shown in Fig. 4 for different wave speeds v, which range from a value close to v_{min} (1.02 c_0), up to v_{max} (1.13 c_0). One observes that the peak strain markedly increases with the wave speed, while the wave width slightly reduces.

Table 1: Predictions of the tensegrity-like model for the velocity and amplitude of rarefaction pulses traveling in a mass-spring chain with softening response, compared to the numerical results presented in [7].

peak amplitude $\phi^* + \epsilon_0(1-\phi^*)$		wave speed	wave width
0.122	Present model	1.02 c_0	10.13 h_0
	Reference [7]	1.00 c_0	12.00 h_0
0.040	Present model	1.10 c_0	6.79 h_0
	Reference [7]	1.08 c_0	10.00 h_0
0	Present model	1.13 c_0	6.10 h_0

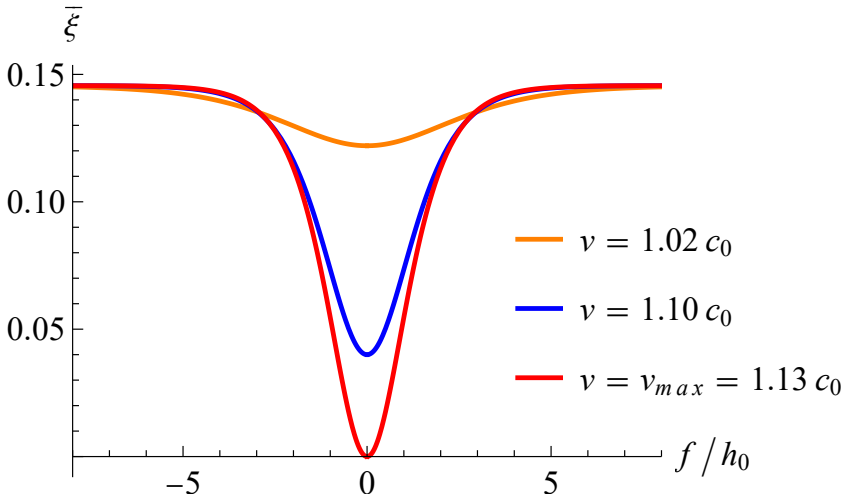

Figure 4: Shapes of the rarefaction pulses predicted by the tensegrity-like model for different values of the wave speed.

6. Concluding remarks

By deriving the quasi-continuum limit of the equations of motion of a tensegrity-like model of a mass-spring system with softening-type response, and conducting an analysis *à la* Weierstrass [12,13], we have predicted the occurrence of rarefaction pulses in chains formed by pre-compressed tensegrity units and lumped masses. The presented results confirm those obtained through a different analytic approach in [8], as well as the numerical results presented in [7] for tensegrity mass-spring chains formed by a large number of units. It is worth noting that the presence of rarefaction pulses in tensegrity mass-spring chains paves the way to the development of a radically new concept for the protection of bodies from the effects of compressive disturbances, which makes use of the solitary wave dynamics of such systems, without necessarily requiring the dissipation of mechanical energy. Such 'metamaterial' behaviors of tensegrity lattices will be studied through future research, in association with bandgap-type responses [15] and superelastic effects [16]. Another potential avenue for future research involves studying the dynamics and stability of innovative transversely isotropic metamaterials consisting of tensegrity chains embedded in a porous matrix [17,18].

Acknowledgements

JdCM acknowledges support by the Italian National Group of Mathematical Physics (GNFM), and the 'Istituto Nazionale di Alta Matematica Francesco Severi' (INdAM).

Funding

This research has been funded under the National Recovery and Resilience Plan (NRRP), by the European Union - NextGenerationEU, within the project with grant number P2022CR8AJ (FF PI). FF also acknowledges funding from the NextGenerationEU PRIN2022 by the NextGenerationEU PRIN2022 research project with grant number 20224LBXMZ ("Ricerca finanziata dall'Unione Europea - Next Generation EU"). Financial support was also received by the Italian Ministry of Foreign Affairs and International Cooperation within the Italy-USA Science and Technology Cooperation Program 2023-2025, Project "Next-generation green structures for natural disaster-proof buildings" (grant no. US23GR15).

References

1. R. E. Skelton and M. C. De Oliveira, *Tensegrity systems*, vol. 1. Springer, 2009.
2. F. Fraternali, G. Carpentieri, and A. Amendola, On the mechanical modeling of the extreme softening/stiffening response of axially loaded tensegrity prisms, *Journal of the Mechanics and Physics of Solids*, vol. 74, pp. 136–157, 2015.
3. D. De Tommasi, G. Puglisi, and F. Trentadue, Tunable shear stiffness in a metamaterial sheet, *Meccanica*, vol. 54, pp. 2029–2037, 2019.
4. A. Micheletti, G. Ruscica, and F. Fraternali, On the compact wave dynamics of tensegrity beams in multiple dimensions, *Nonlinear Dynamics*, vol. 98, no. 4, pp. 2737–2753, 2019.
5. A. Amendola, An analytic study on the properties of solitary waves traveling on tensegrity-like lattices, *International Journal of Non-Linear Mechanics*, vol. 148, p. 104264, 2023.
6. J. de Castro Motta, K. Garanger, and J. J. Rimoli, Propagation of compression solitary waves on tensegrity-like lattices made of truncated octahedrons, *International Journal of Non-Linear Mechanics*, vol. 162, p. 104716, 2024.
7. F. Fraternali, G. Carpentieri, A. Amendola, R. E. Skelton, and V. F. Nesterenko, Multiscale tunability of solitary wave dynamics in tensegrity metamaterials, *Applied Physics Letters*, vol. 105, no. 20, 2014.
8. J. de Castro Motta, F. Fraternali, and G. Saccomandi, Rarefaction pulses on tensegrity lattices are just sech^2-solitary (dark) waves, *Meccanica*, 2024, Submitted for publication.
9. A. Spadoni and C. Daraio, Generation and control of sound bullets with a nonlinear acoustic lens, *Proceedings of the National Academy of Sciences*, vol. 107, no. 16, pp. 7230–7234, 2010.
10. P. A. Clarkson and M. D. Kruskal, New similarity reductions of the boussinesq equation, *Journal of Mathematical Physics*, vol. 30, no. 10, pp. 2201–2213, 1989.
11. P. Rosenau, Dynamics of nonlinear mass-spring chains near the continuum limit, *Physics Letters A*, vol. 118, no. 5, pp. 222–227, 1986.
12. M. Destrade, G. Gaeta, and G. Saccomandi, Weierstrass's criterion and compact solitary waves, *Physical Review E*, vol. 75, no. 4, p. 047601, 2007.
13. G. Saccomandi, Elastic rods, Weierstrass' theory and special travelling waves solutions with compact support, *International Journal of non-linear Mechanics*, vol. 39, no. 2, pp. 331–339, 2004.
14. N. W. Ashcroft and N. D. Mermin, *Solid State Physics*. Holt-Saunders, 1976.
15. L. Placidi, J. de Castro Motta, and F. Fraternali, Bandgap structure of tensegrity mass-spring chains equipped with internal resonators, *Mechanics Research Communications*, p. 104273, 2024.
16. F. Fraternali and J. de Castro Motta, Mechanics of superelastic tensegrity braces for timber frames equipped with buckling-restrained devices, *International Journal of Solids and Structures*, vol. 281, p. 112414, 2023.
17. A. Amendola, J. de Castro Motta, G. Saccomandi, and L. Vergori, A constitutive model for transversely isotropic dispersive materials, *Proceedings of the Royal Society A*, vol. 480, no. 2281, p. 20230374, 2024.
18. J. de Castro Motta, V. Zampoli, S. Chiriţă, and M. Ciarletta, On the structural stability for a model of mixture of porous solids, *Mathematical Methods in the Applied Sciences*, vol. 47, no. 6, pp. 4513–4529, 2024.